E-ISSN: 2528-388X
P-ISSN: 0213-762X

INERSIA
Vol.19, No.2, December 2023

The Mechanism of Rainfall-Induced Landslide Around Railway Tracks in Central Java Province, Indonesia

Ika Sakti Octaviarini[a*], Teuku Faisal Fathani[a], Hary Christady Hardiyatmo[a], Anisa Nur Amalina[b], and Egy Erzagian[a]

[a] Department of Civil and Environmental Engineering, Faculty of Engineering, Universitas Gadjah Mada, Yogyakarta 55281, Indonesia
[b] Department of Civil Engineering, Faculty of Civil Engineering and Planning, Islamic University of Indonesia, Yogyakarta 55584, Indonesia

Keywords:
Mass movement
Rainfall intensity
Water infiltration
Remote sensing
Tension crack

ABSTRACT

Landslide is one of the most disastrous natural hazards in Indonesia, causing significant fatalities and economic losses. Landslides can be triggered by several factors, such as rainfall, earthquakes, soil conditions, and others, where each landslide event has its own triggering and controlling factors. A progressive landslide occurred on the Central Java railway line which resulted in damage to the double-track railway as a transportation infrastructure. The objective of this paper is to understand the process and triggering factors of the landslide. Information was collected through field investigations and measurements based on drilling results at 3 points, geophysical surveys at 5 lines, and laboratory testing of several soil samples. Geological and geotechnical settings, topography, lithology, hydrogeology, and rainfall data of the area were analyzed. Aerial photographs and other remote sensing data were used to evaluate and discuss the information. Landslides in the study area occurred in stages, starting with the formation of a tension crack, followed by two landslides over five months. The results show that the clay material that dominates the study area is the dominant controlling factor of a landslide, triggered by long-duration, low-intensity rainfall. Rainwater entering through tension cracks increases moisture content, adding load to the slope and triggering landslides. Furthermore, the train's external load on the slope also contributes to the occurrence of landslides. The static and cyclic load of the train causes changes in the slope's pressure balance, generating a force that drives the downslope soil. Further analysis was performed using back analysis method with the limit equilibrium method to enhance understanding of slope stability parameters at the time of slope failure. The analysis was performed considering the rising groundwater level. A factor of safety (FS) value of 0.989 was obtained at the end of the simulation, indicating that the slope had failed.

1. Introduction

A landslide is a geological phenomenon where a mass of rock and soil slides along a slope and has occurred in many areas around the world. Landslide disasters cause economic losses and fatalities. From 1981 to 2007, more than 1,000 landslide disasters were reported in the most populated island of Java, with the number of people affected by landslides being more than thousands [1][2]. The high number of casualties due to landslides in Indonesia is caused by the large population of people living in landslide-prone areas [1]. Moreover, Indonesia's climatic (frequent and high-intensity rainfall), geographic (mountainous regions), and geological (located at the junction of three tectonic plates) conditions make it more susceptible to landslides [3][4].

A complex interaction of multiple factors is a major cause of most landslide events, including dynamic events such as heavy rainfall and seismic events; ground conditions such as slope, geology, and soil type; and human disturbances such as de-vegetated slopes and road cuts [5][8]. In general, landslides can be triggered by two main factors: seismic activity by earthquakes [9][10] and rainfall [11][12]. Landslides caused by rainfall are generally caused by changes in pore water pressure resulting in slope instability. An increase in pore water pressure leads to a reduction of soil shear strength. These conditions are often caused by a rise in the groundwater table [13][14][15], an increase in soil saturation [16][17], or the formation of a perched water table [18]. The occurrence of landslides due to rainfall was related to rainfall intensity, slope, and soil composition [19].

*Corresponding author.
E-mail: ikasakti@mail.ugm.ac.id

https://dx.doi.org/10.21831/inersia.v19i2.66835
Received October 21st 2023; Revised December 29th 2023; Accepted December 30th 2023
Available online December 31st 2023

One recorded landslide event occurred gradually in Central Java Province from January to June 2022. The landslide occurred on a slope south of the double-track railway. Landslides that occurred in June 2022 had the most significant impact and affected the main southern railway track with landslide material sliding down the slope toward the river. It has been classified as a shallow slope failure type and presumably triggered by rainfall. The presence of a river at the slope base was also indicated as one of the triggering factors for landslides. The east-west river flow was interpreted as continuously eroding the slope base to the north and south, resulting in the occurrence of landslides along the river banks. In this study, the characteristics of the landslide event are investigated in detail through field investigations and data interpretation. The causes and triggers of the landslide are analyzed.

2. Description of Landslide

2.1 General Introduction

A landslide was reported on the southern side of the double-track railway in Central Java Province shown in Figure 1. The landslides occurred gradually from January to June 2022. However, the landslide that occurred in June 2022 had the most significant impact, causing subsidence on the railway tracks, especially on the southern side. The occurrence of the landslide resulted in the disruption of train operations, as the train had to operate below the operational speed when passing through the landslide area. The trains operating speed under normal conditions reached 110 km/hour, but after the landslide occurred, the speed of passing trains had to be reduced to 60 km/hour for the northern railway line and 20 km/hour for the south. The landslide had a crown with dimensions 38 meters long and 12 meters high, and the coverage area reached 984 m^2 shown in Figure 2. Its movement mechanism was rotational sliding with landslide material consisting of a mixture of soil, sand, clay material, and vegetation.

2.2 Geological and Geotechnical Settings

Soil investigation was carried out at the study area using the standard penetration test method and soil sampling for further laboratory testing to determine soil engineering properties, as seen in Figure 3. There were also five geoelectrical testing lines. The geoelectrical survey is a method for interpreting the characteristics of rock and structure below the soil surface by utilizing electrical properties.

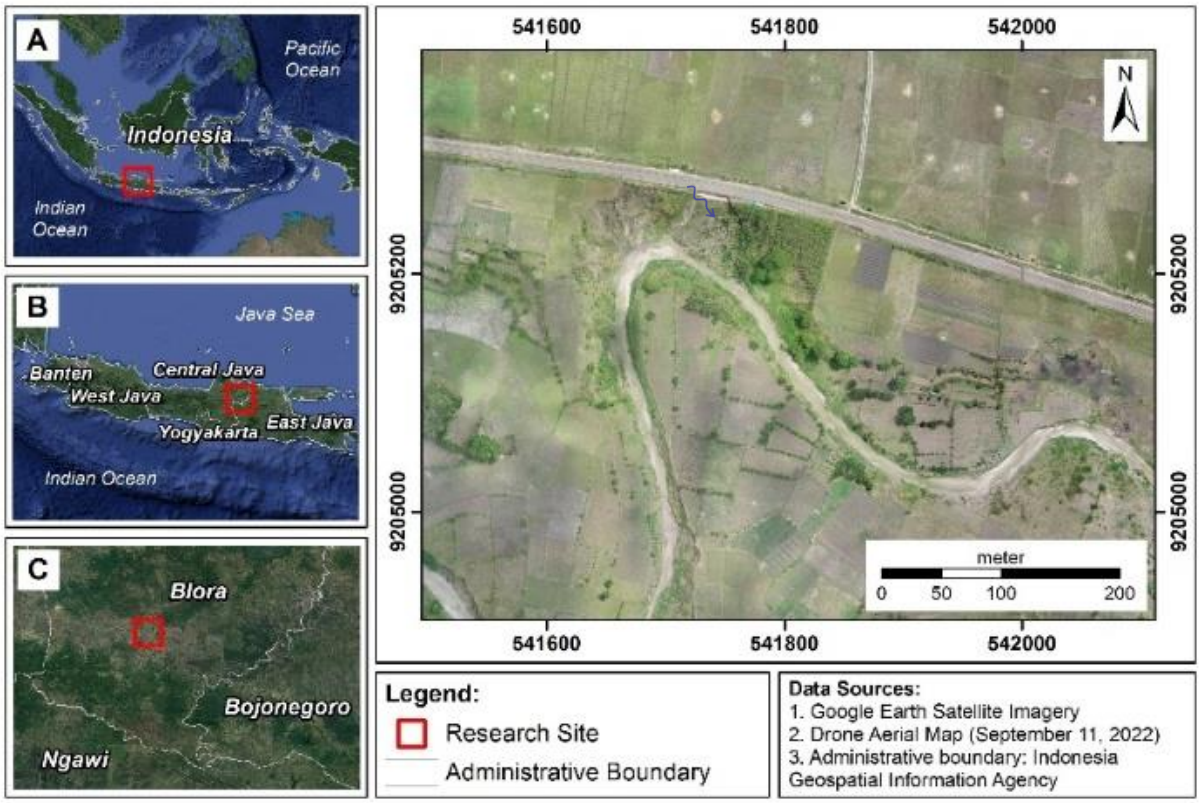

Figure 1. Study area.

Figure 2. Landslides in the study area.

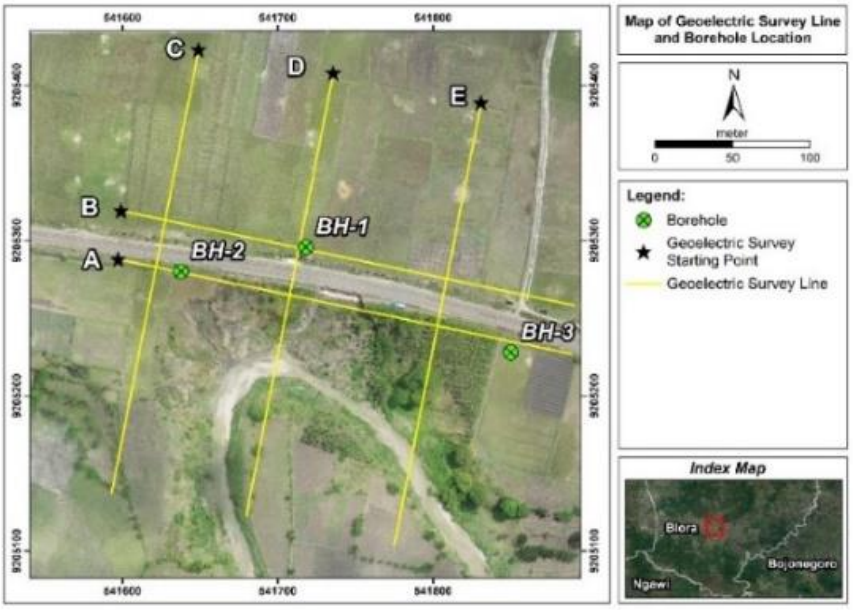

Figure 3. Geoelectrical line and borehole point map.

The SPT results indicated that the soil layer was predominantly composed of clay with an N-SPT value of less than 30 up to a depth of 30 meters at all three locations. The clay layer had a consistency ranging from soft to very stiff. A longitudinal soil stratigraphy was made through the three borehole points (lines A-A') to determine the subsurface layering at the study area shown in Figure 4.

Soil samples obtained from borehole testing were tested in the laboratory with several series of soil tests to determine the physical and mechanical properties of soil layers. According to the Unified Soil Classification System (USCS), soil samples were classified as high-plasticity inorganic clay (CH), low-plasticity clay (CL), low-plasticity clay (MH), and clayey sand (SC). In general, soil in the study area was dominated by high-plasticity inorganic clay (CH) which was found in most of the soil samples.

A geoelectrical survey was carried out on 2 (two) longitudinal lines on the north and south sides of the railway line and 3 (three) lines transverse to the railway line. The survey was carried out using the electrical resistivity tomography or geoelectrical mapping method in 2D with a dipole-dipole electrode configuration. After processing the data, the results are obtained in the form of 2D subsurface sections shown in Figure 5. In general, the results of geoelectrical measurements can be used to support the SPT results. According to Table 1, clayey soils have a resistivity of 1.5 – 3.0 ohm.m. Alternatively, soft and firm clay can be identified through SPT results. Meanwhile, the resistivity value of 3 – 15 ohm.m is silty soils or the SPT results are stiff and very stiff clay. So, it can be concluded that the resistivity value will be greater

from soft to very stiff clay. This corresponds with the concept of the geoelectric method that the harder a medium is, the higher the resistivity value will be.

The zones that encounter landslides are indicated by line D which extends for 240 m (north-south) with the location of the borehole point (BH-1) at a distance of approximately 100 m. In general, the type of soil based on the resistivity cross-section on path D consists of three types, namely soft clay (about 2 ohm.m), stiff clay (3 – 4 ohm.m), and very stiff clay (>5 ohm.m). The grouping of soil types is correlated with the results of borehole testing so that geoelectric data can support the results of borehole data interpretation. The landslide area has surface soil that is dominated by soft clay where these zones are described with low resistivity values (about 2 ohm.m) which are soft clay. This follows the theory of the geoelectric method that the landslide zone will occur in a medium with a low resistivity value.

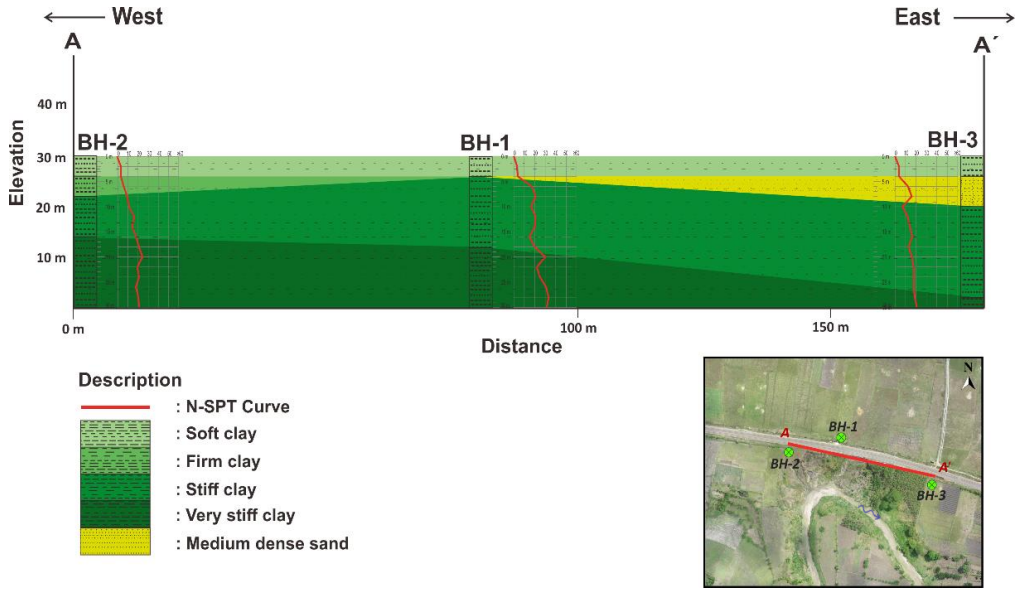

Figure 4. Soil stratigraphy.

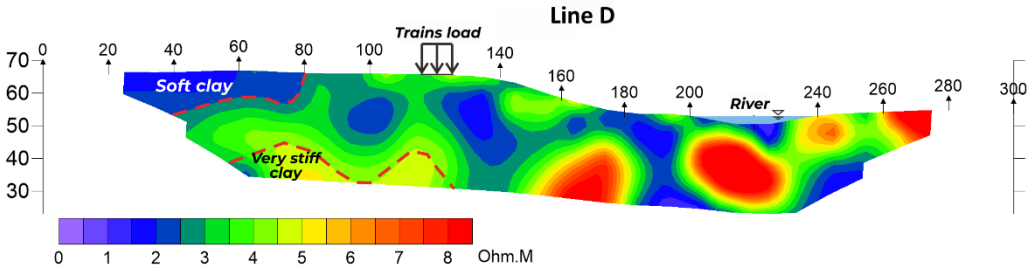

Figure 5. Geoelectrical survey results at line D.

Table 1. Typical resistivity values for geologic materials [20].

Materials	Resistivity	
	Ω ft	Ω m
Clayey soils: wet to moist	5 – 10	1.5 – 3.0
Silty clay and silty soils: wet to moist	10 – 50	3 – 15
Silty and sandy soils: moist to dry	50 – 500	15 – 150
Bedrock: well fractured to slightly fractured with moist soil-filled cracks	500 – 1000	150 – 300
Sand and gravel with silt	About 1000	About 300
Sand and gravel with silt layers	1000 – 8000	300 – 2400
Bedrock: slightly fractured with dry soil-filled cracks	100 – 8000	300 – 2400
Sand and gravel deposits: coarse and dry	>8000	>2400
Bedrock: massive and hard	>8000	>2400
Freshwater	67 – 200	20 – 60
Seawater	0.6 – 0.8	0.18 – 0.24

[a] From Soilest, Inc.
Note: (1) In soils, resistivity is controlled more by water content than by soil minerals. (2) The resistivity of the pore or cleft water is related to the number and type of dissolved ions and the water temperature.

3. Causes and Triggering Factors

3.1 Geomorphology and Lithology

The study area has elevation profiles ranging from 40 – 60 m. The landslide crown was at 58 m masl at the level of the railway track, with a height difference of ±10 m from the river flow. The slopes throughout the study area are generally flat (0˚ – 3˚). Segments adjacent to the river have slopes ranging from undulating (3˚ – 8˚), moderately sloping (8˚ – 15˚), and hilly (15˚ – 30˚), especially near river banks where landslides have occurred. The geomorphology of this area is an important factor in causing landslides. Slope gradient and slope aspect can influence landslide initiation because gravity acts on the sliding plane of the slope [21]. In addition, the landslide crown was at the river's cut-off point, which may erode due to river flow.

The local lithology is composed of alluvial deposits consisting of unconsolidated material on the body and banks of the river. Based on the rock formation, the alluvial deposits consist of clay, silt, sand, and gravel and were deposited along the floodplain of the Lusi River. Clay material which dominates in the research area is proven by the results of the soil investigation that has been described previously. Slopes with clay soil that have low permeability will inhibit the water in the body of the slope from exiting, it will result in an additional load on the slope and triggering instability. In dry conditions, clay material is highly susceptible to shrinkage and cracking (this is especially true for clay materials with high plasticity). After rainfall, shrinkage cracks appeared, allowing rainwater to infiltrate the topmost few meters of the slope crest. Due to the low permeability, water movement downwards was stopped, resulting in a perched water zone forming near the slope's crest. The presence of water causes soil to lose its shear strength and create a weak zone along the cracks.

3.2 Hydrogeology

The study area is the downstream part of the perennial river of the Jampi River and a tributary river of the Lusi River in the northwest shown in Figure 6. The river valley is located south of the main rail line and is classified as an old stadia. According to [22], the mature to old stadia areas are characterized by rivers in this section dominated by "U" shaped valleys and show indications of lateral erosion, which are slow but more dominant than vertical erosion. This is also supported by evidence of a lateral shift of river water flow.

Based on the results of a comparison between aerial photographs and available Google Earth satellite imagery, information is obtained that the river bends are being naturally displaced. Changes in the river bend from 2000 to 2022 can be seen in Figure 7. In 2000, the riverbank was ±50 m south of the railway tracks. The shape of the river bend has shifted, tapering more and more to the north, causing the riverbank to move closer to the railway tracks. In 2022, the riverbank will be approximately 45 m south of the railway tracks, indicating a shift of up to 5 meters north or approaching the railway tracks. Thi and Minh (2019) reported that soil erosion may cause riverbanks to become increasingly overhanging [23]. During the rainy season, the river water level rises, resulting in a high shear stress flow that expands the width of soil erosion and creates an overhanging bank shape.

Figure 6. River conditions in the study area

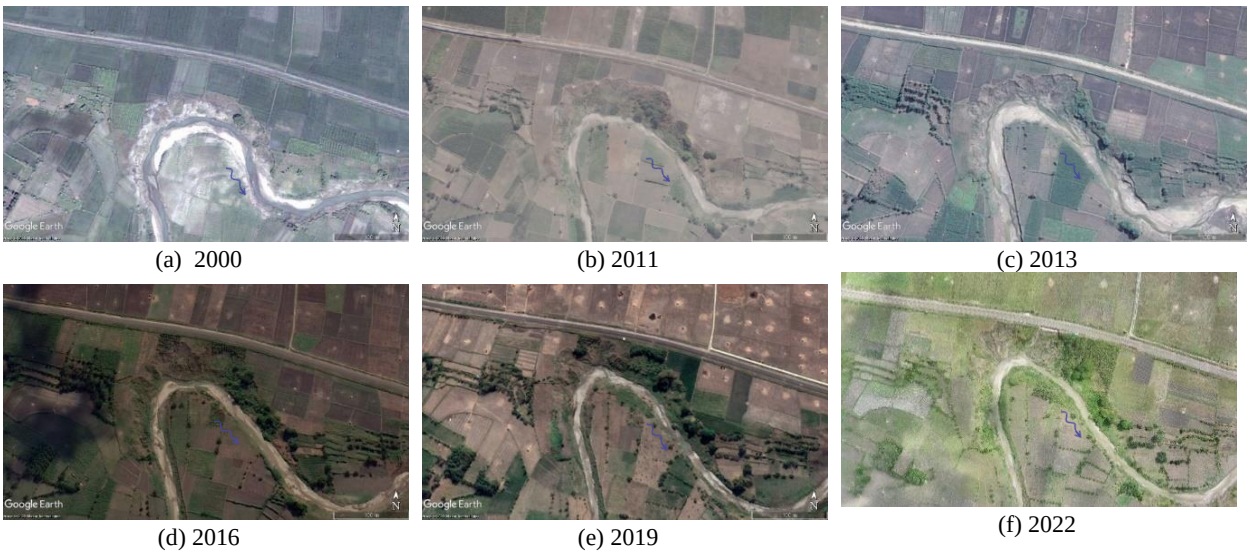

(a) 2000 (b) 2011 (c) 2013

(d) 2016 (e) 2019 (f) 2022

Figure 7. Changes in river bend [24].

Soil erosion significantly impacts riverbank stability and is caused by hydraulic dynamic [25][26] and seepage erosion [27]. Bank instability can lead to mass failure through various combinations of weakening factors, i.e. those processes that act on the bank material to reduce its strength, and a variety of erosion processes. The surrounding areas are characterized by cliffs, which are susceptible to landslides caused by erosion that erodes the cut-off slope, with avalanche material moving toward the river valley in the south.

3.3 Long-duration, Low-intensity Rainfall

The landslide that occurred in the study area was a progressive landslide, with tension cracks forming on the slope on 26 January 2022 shown in Figure 8. The cracked soil gradually became unstable and moved down the slope, resulting in a landslide on May 9, 2022. The landslide area expanded causing subsidence on the south side of the railway line on June 30. Although landslides can be influenced by several factors such as slope conditions and angle, lithology, soil type, and hydrological or meteorological conditions [28], rainfall is considered to be the main trigger for landslides in the study area. This is because most of the landslides reported in the area occurred during months of intense rainfall. The measurement of water that falls on the ground during a specific period is expressed in millimeters (mm) through rainfall. The 2022 hourly rainfall record was obtained from meteorological stations maintained by the Japan Aerospace Exploration Agency (JAXA). Figure 9 shows the distribution of daily rainfall over 6 months in the study area.

It rained on 11 days between January 7 and January 22 with an intensity of 7.94 – 58.08 mm/day before the slope area experienced massive cracks. The total cumulative rainfall that occurred from January 1 to 25 was 220 mm, indicating a long duration of rainfall and low intensity in that period. A major landslide occurred on May 9, 2022, approximately three months after the tension cracks formed. During that period, more than 45 rainfall ranging from 6.00 – 47.84 mm/day with a rainfall duration of 1 – 11 hours were recorded.

(a) (b)

Figure 8. Landslide event time: (a) January 26; and (b) May 9 [29].

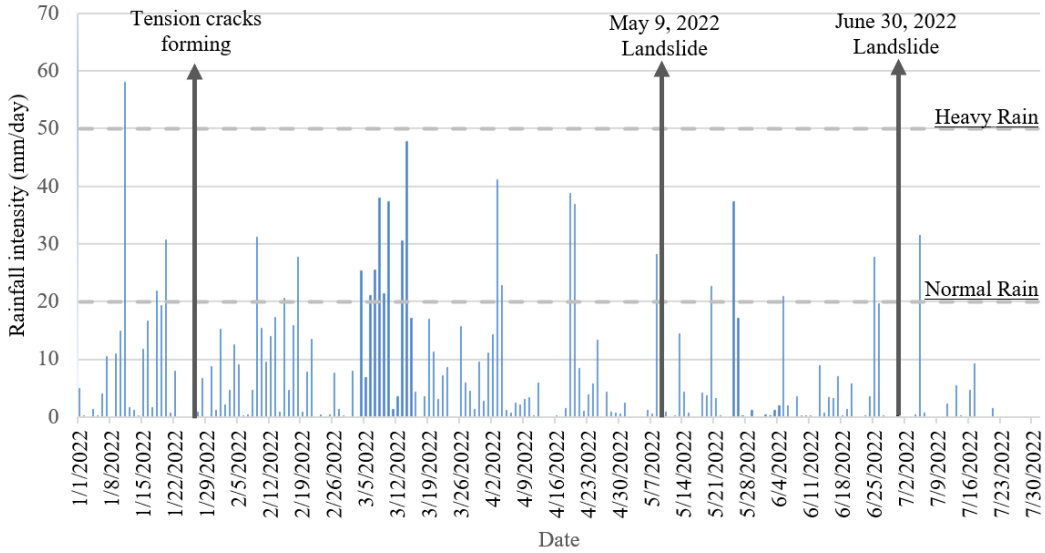

Figure 9. Daily precipitation data from January to June

The second landslide had a larger coverage area than the first. This landslide caused the soil mass on the south side of the railway line to collapse and resulted in the subsidence of the railway tracks. The landslide on June 30 occurred less than two months after the initial one. During that period, there were around 11 light to normal rain events with continuous rain lasting between 1 – 7 hours.

Based on rainfall data and the chronology of landslide events described above, it can be seen that landslides did not occur immediately after the highest rainfall intensity. Landslides in the study area occurred after continuous rainfall events, with the time for landslide occurrence 1 – 4 months after the first rain. This is supported by the results of research from Zeˆzere et al. (2005), which suggested antecedent rainfall of 1 – 15 days for shallow landslides and 1 – 3 months for deep-seated failure [30].

3.4 Train load

The railway line in the study area is an important transportation infrastructure connecting several regions in Central Jawa. The train on this line is designed for passengers and freight, with a maximum speed of 110 km/h and a locomotive weight of up to 90 tons. Live traffic loads from high-speed trains place additional loads on the slope, which can trigger slope failure due to changes in the pressure balance in the slope body and create a driving force on the downslope soil. The soil layer directly under the track is the area most affected by the train load. This area can be used to clearly illustrate the state of load transfer and accumulation of deformation, which can assess the development of slope failure. The dynamic force acting on the rail results in the track vibrating and creating a dynamic interaction between each sleeper and the ballast. The long-term stability of the slope will be negatively affected by the cyclic dynamic load induced by train operation. The vibration load of trains causes deformation and damage to railway slopes. When a train passes, the slope may develop micro-cracks and become unstable [31]. According to Xi et al. (2020), as the heavy-duty train moves along the track, it generates a constant vibration that is transmitted through the rail, sleeper, and ballast to the supporting structure [32]. These vibrations are then transmitted to the subgrade and slope in the form of vibration waves. The safety and stability of the surrounding area can be significantly impacted by the high amplitude and long-duration vibrations caused by heavy trains.

4. Movement Mechanism

All the landslide events did not occur during the highest daily rainfall. The first landslide did not occur immediately after high-intensity rain on January 11, 2022, with an intensity reaching 58 mm/day but rather occurred several months after the heavy rain. Based on this phenomenon, the amount of rainfall in one day is not the only factor that triggers slope instability, but prolonged rainfall may play a role in developing the mechanism for landslides.

The mechanism of landslides is influenced not only by the duration of rain but also by the type of soil. The soil in the research area is composed of clay, which has a low permeability coefficient. As a result, rainwater will take a longer time to infiltrate the soil and will be stored in it for an extended period. This will lead to the creation of a perched water zone near the crest of the slope. Slopes with low-permeability soil are likely to fail during prolonged rainfall, while those with high-permeability soil are less susceptible [33].

In the period after the formation of tension cracked and before the landslide occurred, more than 45 rain events were recorded with a fairly long duration. Rainwater infiltrates and accumulates in the slope through the tension cracks that form, generating lateral water pressure that creates horizontal pressure. Furthermore, rainwater infiltration contributes to the loss of suction and a decrease in effective stress, causing the soil mass to weaken and become unstable. Due to lateral water pressure, uplift pressure, and soil softening, the slip surfaces merge completely in the sliding zone and the unstable soil mass immediately collapses, which is the initiation of a landslide shown in Figure 10.

The movement of material causes the slope to become more upright and in unstable conditions. The second landslide occurred 2 months after the first landslide occurred. During this period, rain was recorded with light to normal intensity. As the rain continues to fall, rainwater will enter the body of the slope, increasing the load on the slope and causing the slope to become unstable. Rainwater that enters the soil will reduce the shear strength of the soil. This worsens the already unstable condition of the slopes. The reduction in shear strength leads to a decrease in the slope's factor of safety and subsequently triggers landslides. A schematic of the movement mechanism of slope failure in the study area is given in Figure 11.

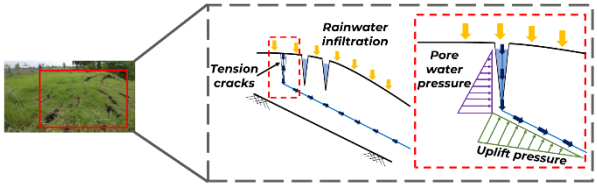

Figure 10. Water pressure distribution in tension cracks.

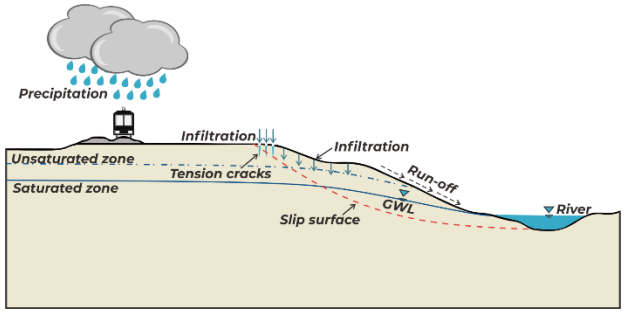

Figure 11. The mechanism of slope failure in the study area.

5. Numerical Simulation

A slope failure implies that the factor of safety of the slope at the moment of failure is unity. Back analysis is commonly used to improve understanding of slope stability parameters, such as soil shear strength and pore water pressure at the time of slope failure [34]. Determination of slope geotechnical properties using back analysis techniques and slope stability analyses was performed using 2-D limit equilibrium slope stability program. In the limit equilibrium formulation, it is assumed that the soil behaves similarly to Mohr-Coulomb material. The cohesive and frictional components of strength have equal factors of safety (FS) for all soils involved, and the FS remains consistent for all slices [35].

Back analysis is performed to produce FS values that are in line with field conditions. In determining slope stability, the term FS is defined as the ratio of the resistance moment to the moment that moves the soil mass in the landslide area. The FS value determines the slope stability condition. The categories are shown in Table 2.

Table 2. FS value categories for slope stability [36].

FS	Condition
< 1.07	Landslide occurred
1.07 < FS < 1.25	Landslide can occur
> 1.25	Landslides rarely happen

The slope stability analysis was performed with SLOPE/W using the Morgenstern-Price method. Landslide simulation was started with the slope geometrics determination at the most critical cross-section. The simulation was performed with five different groundwater level scenarios. The first simulation modeled the groundwater level below the riverbed since the river is dry during the dry season according to local conditions. Figure 12b shows the results of this simulation, which produced an FS value of 1.288. In the second simulation, the groundwater level slowly rose due to the infiltration of rainwater into the soil and reached approximately 4.5 meters above the first water level, as shown in Figure 12b. The simulation results of the second scenario produced an FS value of 1.185.

In the third simulation, the groundwater level was at a depth of 4.5 below the ground surface shown in Figure 12c. The simulation results showed a factor of safety (FS) of 1.093. However, based on Table 2, this FS value is lower than the minimum required value of 1.25, indicating a potential for landslides. This is due to the formation of tension cracks that make the slope unstable. As a result, there is a high risk of landslides. This condition is the beginning of a slope-critical condition.

In the next simulation, the groundwater level was at a depth of 2 m from the ground surface and gives an FS value of 1.054 shown in Figure 12d. It is important to note that the FS value will decrease as the groundwater level rises. In the last simulation, the groundwater level was at a critical condition or the soil was fully saturated shown in Figure 12e. The slope stability analysis results showed an FS value of 0.989 indicating that the slope had already failed and experienced a landslide. This result is in line with the field conditions where the slope is located.

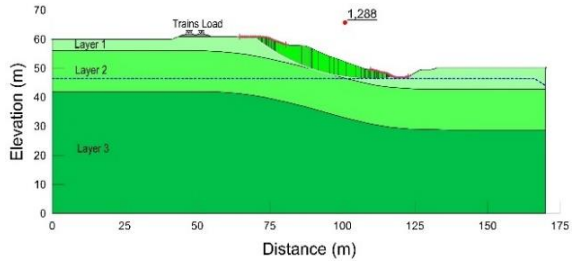

(a)

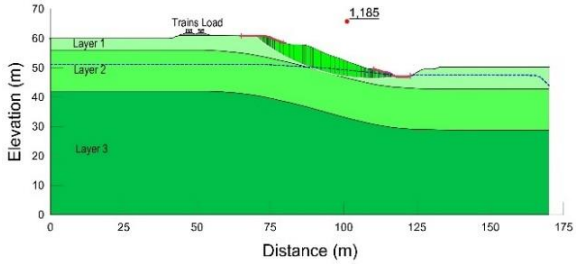

(b)

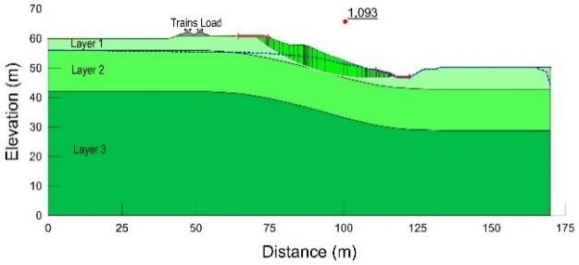

(c)

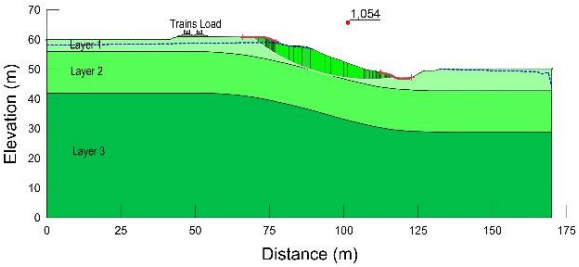

(d)

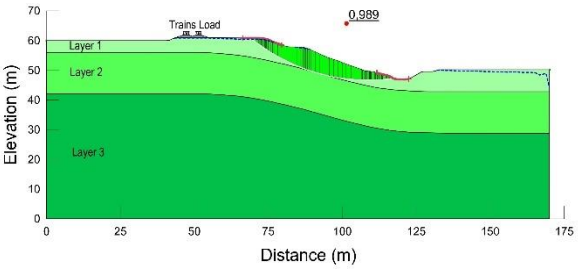

(e)

Figure 12. Simulation results.

6. Conclusion and Recommendations

The triggering mechanism and background of this landslide were thoroughly analyzed shortly after it occurred. Hence, the following conclusions can be drawn.

Landslides in the study area can be classified as rotational landslides that had a crown of 38 meters in length, 12 meters in height, and a coverage area of 984 m². The landslide disrupted the rail transportation network that crossed the railway line on the upper side of the slope. The landslide that occurred can be described as a progressive landslide which started with the formation of a tension crack on the slope and was followed by the first landslide occurring 3 months apart. Subsequently, a second and larger landslide took place in less than 2 months.

The soil at the landslide location is dominated by clay material with high plasticity. Clay, a weathering product of rock, can contribute to landslides due to its chemical and physical properties [37]. Due to the low permeability, water movement downwards was stopped. As a result, a perched water zone forms near the crest. The presence of water weakens the soil's shear strength, creating a weak zone along the cracks.

Based on the chronology of landslide events and rainfall data, it can be observed that landslides are more influenced by antecedent rainfall rather than the highest rainfall intensity. Continuous rainfall resulted in water retention at the top of the hill and created a high saturation in the soil, causing infiltration where water enters the pores of the soil until it comes into contact with the bedrock [38].

The train load acting on the slope also plays a role in the mechanism of landslides. The maximum speed of the train on this line is 110 km/h, and it is designed to carry both passengers and freight. The locomotive can weigh up to 90 tons. Passing trains provide additional load on slopes, besides that, live traffic from high-speed trains can trigger slope failure due to pressure imbalances and create a driving force on downslope soil.

Back analysis is performed to better understand slope stability parameters such as soil shear strength and pore water pressure at the time of slope failure. Based on the results of numerical simulation, it is obtained that the FS value decreases as the groundwater level increases. The FS value obtained was 0.989 when the landslide occurred

The results of the back analysis, in the form of soil shear strength, can be used to design appropriate mitigation measures for slopes that have failed. These measures can be categorized as control works and restraint works. Control works include modification of slope geometry and infiltration control during rainfall. On the other hand, restraint works include the construction of retaining walls, piles, geosynthetics, anchors, etc.

Acknowledgments

The author would like to thank the Center for Disaster Mitigation and Technological Innovation Universitas Gadjah Mada (Gama-InaTEK) and PT Kereta Api Indonesia (Persero) for supporting field investigation and providing valuable advices.

References

[1] D. S. Hadmoko, f. Lavigne, j. Sartohadi, p. Hadi dan winaryo, "landslide hazard and risk assessment and their application in risk management and landuse planning in eastern flank of menoreh mountains, yogyakarta province, indonesia," *natural hazards*, vol. 54, pp. 623-642, 2010.

[2] J. Cepeda, h. Smebye, b. Vangelsten, b. Nadim dan d. Muslim, "landslide risk in indonesia, global assessment report on disaster risk reduction," isdr, 2010.

[3] S. S. Kyi, t. D. Nguyen, k. Aoki, y. Mito, k. B. Suryolelono, d. Karnawati dan s. Pramumijoyo, "landslide risk microzonation by using multivariate statistical analysis and gis," *nt. J. Jpn. Comm. Rock mech*, vol. 3, no. 1, pp. 7-15, 2007.

[4] Z. Umar, b. Pradhan, a. Ahmad, m. N. Jebur dan m. S. Tehrany, "earthquake induced landslide susceptibility mapping using an integrated ensemble frequency ratio and logistic regression models in west sumatera province, indonesia," *catena*, vol. 118, pp. 124-135, 2014.

[5] M. J. Haigh, j. S. Rawat, m. S. Rawat, s. K. Bartarya dan r. P. Rai, "interactions between forest and landslide activity along new highways in the kumaun himalaya," *forest ecology and management*, vol. 78, no. 1-3, pp. 173-189, 1995.

[6] M. T. J. Terlien, "he determination of statistical and deterministic hydrological landslide-triggering thresholds," *environmental geology*, vol. 35, pp. 124-130, 1998.

[7] S. Bai, j. Wang, r. Bell dan t. Glade, "distribution and susceptibility assessments of landslide triggered by wenchuan earthquake at longnan," melbourne, australia, 2012.

[8] J. W. Zhou, p. Cui dan x. G. Yang, "dynamic process analysis for the initiation and movement of the donghekou landslide-debris flow triggered by the wenchuan earthquake," *journal of asian earth sciences*, vol. 76, pp. 70-84, 2013.

[9] X. Fan, g. Scaringi, q. Xu dan w. Zhan, "coseismic landslides triggered by the 8th august 2017 ms 7.0 jiuzhaigou earthquake (sichuan, china): factors controlling their spatial distribution and implications for the seismogenic blind fault identification," *landslides*, vol. 15, no. 5, pp. 967-983, 2018.

[10] R. Kusumawardani, m. Chang, t. C. Upomo, r. C. Huang, m. H. Fansuri dan g. A. Prayitno, "understanding of petobo liquefaction flowslide by 2018.09. 28 palu-donggala indonesia earthquake based on site reconnaissance," *landslides*, vol. 18, p. 3163–3182, 2021.

[11] N. Luo, r. J. Bathurst dan s. Javankhoshdel, "probabilistic stability analysis of simple reinforced slopes by finite element method," *computers and geotechnics*, vol. 77, no. 7, pp. 45-55, 2016.

[12] Q. Ran, y. Hong, li dan j. Gao, "a modelling study of rainfall-induced shallow landslide mechanisms under different rainfall characteristics," *journal of hydrology*, vol. 563, no. 8, pp. 790-801, 2018.

[13] J. Corominas, j. Moya, a. Ledesma, a. Lloret dan j. A. Gili, "prediction of ground displacements and velocities from groundwater level changes at the vallcebre landslide (eastern pyrenees, spain)," *landslides*, vol. 2, p. 83–96, 2005.

[14] R. Rosso, k. M. Rulli dan g. Vannucchi, "a physically based model for the hydrologic control on shallow landsliding," *water resources research*, vol. 42, no. 6, 2006.

[15] E. Conte, a. Donato, l. Pugliese dan a. Troncone, "analysis of the maierato landslide (calabria, southern italy)," *landslides*, vol. 15, p. 1935–1950, 2018.

[16] D. Salciarini, j. W. Godt, w. Z. Savage, r. L. Baum dan p. Conversini, "modeling landslide recurrence in seattle, washington, usa," *engineering geology*, vol. 102, no. 3–4, pp. 227-237, 2008.

[17] E. Conte dan a. Troncone, "simplified approach for the analysis of rainfall-induced landslide," *journal of geotechnical and geoenvironmental engineering*, vol. 138, p. 398–406, 2012.

[18] C. D. Shackelford, c. K. Chang dan t. F. Chiu, "the capillary barrier effect in unsaturated flow through soil barriers," edomonton, ab, canada, 1994.

[19] Y. Liu, z. Deng dan x. Wang, "the effects of rainfall, soil type and slope on the processes and mechanisms

of rainfall-induced shallow landslides," *applied sciences*, vol. 11, no. 24, p. 11652, 2021.

[20] R. E. Hunt, geotechnical investigation methods a field guide for geotechnical engineers, boca raton: crc press , 2007.

[21] J. Torizin, "bivariate statistical method for landslide susceptibility analysis using arcgis," project of technical cooperation "mitigation of georisks" in bogor, bogor, 2011.

[22] A. K. Lobeck, geomorphology, an introduction to the study of landscapes, new york: mcgraw-hill book company, 1939.

[23] T. D. Thi dan d. D. Minh, "riverbank stability assessment under river water level changes and hydraulic erosion," *water*, vol. 11, p. 2598, 2019.

[24] Google earth, 2000-2011-2013-2016-2019-2023. [online]. Available: https://earth.google.com/. [accessed 7 july 2023].

[25] K. Klavon, g. Fox, l. Guertault, e. Langendoen, h. Enlow, r. Miller dan a. Khanal, "evaluating a process-based model for use in streambank stabilization: insights on the bank stability and toe erosion model (bstem)," *earth surface processes and landforms*, vol. 42, p. 191–213, 2017.

[26] M. Jugie, f. Gob, c. Virmoux, d. Brunstein, v. Tamisier, c. Le coeur dan d. Grancher, "characterizing and quantifying the discontinuous bank erosion of a small low energy river using structure-from-motion photogrammetry and erosion pins," *journal of hydrology*, vol. 563, pp. 418-434, 2018.

[27] A. Masoodi, a. Noorzad, m. R. Majdzadeh tabatabai dan a. Samadi, "application of short-range photogrammetry for monitoring seepage erosion of riverbank by laboratory experiments," *journal of hydrology*, vol. 558, p. 380–391, 2018.

[28] F. E. S. Silalahi, pamela, a. Yukni dan h. Fahrul, "landslide susceptibility assessment using frequency ratio model in bogor, west java, indonesia," *geoscience letters*, vol. 6, no. 10, 2019.

[29] Pt java konsul utama, "laporan akhir penanganan daerah rawan km 63+100 s.d 63+200 petak jalan antara stasiun doplang dan stasiun randublatung daop 4 semarang," pt java konsul utama, bandung, 2022.

[30] J. L. Zeˆzere, r. M. Trigo dan i. F. Trigo, "shallow and deep landslides induced by rainfall in the lisbon region (portugal): assessment of relationships with the north atlantic oscillation," *natural hazards and earth system sciences*, vol. 5, p. 331–344, 2005.

[31] Y. Ban, x. Fu dan q. Xie, "revealing the laminar shale microdamage mechanism considering the relationship between fracture geometrical morphology and acoustic emission power spectrum characteristics," *bulletin of engineering geology and the environment*, vol. 79, no. 2, p. 1083–1096, 2020.

[32] Q. Xie, z.-h. Wu, c.-b. He, j. Dong, z.-l. Cao dan l. Liang, "dynamic response and mechanical deformation properties of the soil," *arabian journal of geosciences*, vol. 13, p. 618, 2020.

[33] L. M. Lee, n. Gofar dan h. Rahardjo, "a simple model for preliminary evaluation of rainfall-induced slope instability," *engineering geology*, vol. 108, no. 3-4, pp. 272-285, 2009.

[34] L. L. Zhang, l. M. Zhang dan w. H. Tang, "back analysis of slope failure with markov chain monte carlo simulation," *computers and geotechnics*, vol. 37, pp. 905-912, 2010.

[35] R. Urgeles, d. Leynaud, g. Lastras, m. Canals dan j. Mienert, "back-analysis and failure mechanisms of a large submarine slide on the ebro slope, nw mediterranean," *marine geology*, vol. 226, pp. 185-206, 2006.

[36] J. E. Bowles, physical and geotechnical properties of soil, singapore: mcgraw-hil, 1984.

[37] A. Yalcin, "the effects of clay on landslides: a case study," *applied clay science*, vol. 38, no. 1–2, p. 77–85, 2007.

[38] W. Wilopo dan t. F. Fathani, "the mechanism of landslide-induced debris flow in geothermal area, bukit barisan mountains of sumatra, indonesia," *journal of applied engineering science*, vol. 19, no. 3, pp. 688-697, 2021.